

# Uncertainty Assessment of Calibrated Structured Planar LIF/Mie Ratio-metric Imaging

Andrew Corber<sup>\*1</sup>, Patrizio Vena<sup>1</sup>, Wajid Chishty<sup>1</sup>

<sup>1</sup>Aerospace Research Centre, National Research Council of Canada, Ottawa, Canada

\*Corresponding author: [Andrew.Corber@nrc.ca](mailto:Andrew.Corber@nrc.ca)

## Abstract

Planar droplet sizing techniques, such as laser induced fluorescence (LIF) to Mie ratio imaging, have the potential to capture large amounts of spatially resolved droplet size information quickly. In order to do so reliably however, an accurate calibration is required. This work focuses on the assessment of a Sauter-mean diameter calibration methodology applied to LIF/Mie ratio-metric images. The aim here is to determine the range of applicability of this calibration approach, as well as its effectiveness by determining the uncertainties of the resulting planar droplet size map. The images used to proof this methodology were collected using structured laser illumination planar imaging (SLIPI) on sprays from a simple pressure atomizer under elevated ambient pressures. Three liquids were used in these experiments: nozzle calibration fluid, conventional jet fuel and a high viscosity alternative jet fuel. Fuel flows ranged from 2 g/s to 5 g/s, and the ambient pressure was varied between 1.1 and 10 atm. The results of the study show that this calibration method generates similar calibration curves at a wide range of operating conditions and can be approximated by a logarithmic function. The data also show that the calibration curve is agnostic to the fuel mass flow rate, but is dependent on ambient air pressure.

## Keywords

Planar droplet sizing, SLIPI, LIF/Mie, PDA, PDPA, jet fuel, alternative jet fuel, calibration

## Introduction

Sprays play an important role in many industrial systems such as painting, chemical processing, and combustion. Due to their complex, transient, and multiphase nature, gaining a comprehensive understanding of a spray's flow field presents numerous challenges. Recent developments in the field of optical diagnostics, namely Structured Laser Illumination Planar Imaging (SLIPI), has offered a solution to some of these problems, and has been shown by Berrocal et al. [1] to allow for the successful capture of images that are free of the effects due to the multiple scattered laser light. By using SLIPI to collect simultaneous Mie and Laser Induced Fluorescent (LIF) images, Berrocal et al. [2] [3] showed that an accurate 2D map of the relative droplet Sauter-mean diameter (SMD) could be measured. An example of this relative SMD chart is shown in Figure 1.

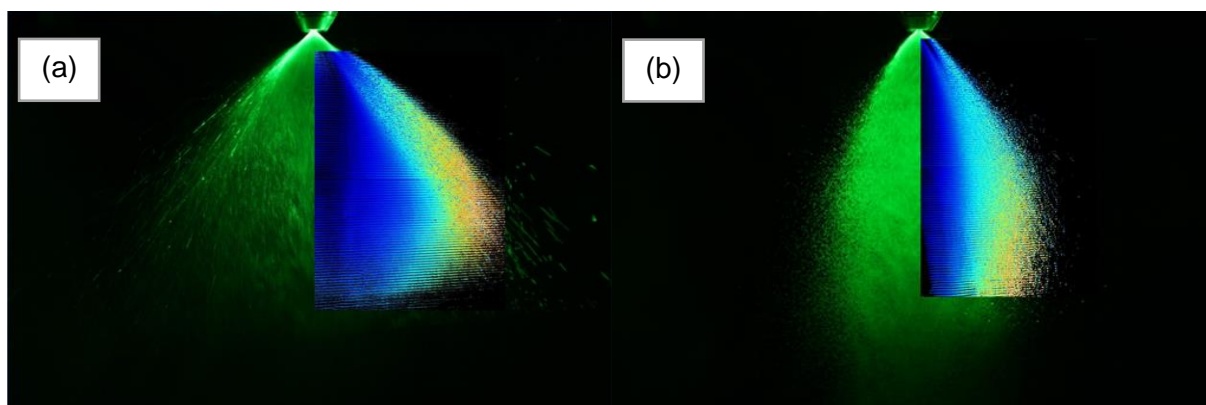


**Figure 1.** Un-calibrated SLIPI LIF/Mie ratio-metric overlaid on conventional laser sheet image of jet fuel spray.  
(a) Ambient air pressure of 1.1 atm fuel flow of 5 g/s. (b) Ambient air pressure of 10 atm, fuel flow of 5 g/s.

In order to generate a map of the absolute droplet SMD's a calibration is required. Mishra et al. [4] demonstrated a successful calibration of a LIF/Mie ratio-metric image using phase Doppler anemometry (PDA). This is a significant advancement since a single LIF/Mie ratio-metric image only takes a few seconds to capture, but contains a prodigious amount of spatially resolved droplet size information. Collecting the same volume of SMD data using PDA would require several hours. In previous work [5], we collected SLIPI LIF/Mie images and made PDA measurements at different axial planes in the spray in order to compare the resulting calibration curves. Our results

showed that in order to produce the best calibration, PDA data should be collected in an area of the spray that offers the largest range of droplet sizes. This work also showed the potential for a single calibration curve to be applied for multiple images. PDA data is time consuming, and therefore expensive to obtain, so having the ability to use a single calibration for multiple LIF/Mie images is a valuable objective. Questions remain however on how widely a calibration could be applied, and what are the resulting uncertainties. This paper aims to address some of these queries by presenting numerous LIF/Mie ratio-metric images calibrated using of PDA data so that the calibration curves can be compared to assess their variability. The results show that for these experiments all calibration curves are well fit by a logarithmic function in which the coefficients trend with ambient pressure.

### Material and methods

All testing was conducted using a simple-orifice type pressure atomizer. It has two flow passage, “pilot” and “main”, with flow numbers (FN) of 0.2 g/s/kPa<sup>1/2</sup> and 1.1 g/s/kPa<sup>1/2</sup> respectively. Only the pilot was used in this campaign, which produces a hollow cone spray. More information about this hardware is given in [5] [6]. Experiments were carried out in the National Research Council of Canada’s (NRC) High Pressure Spray Facility (HPSF) in Ottawa, Canada. This test platform consists of an optically accessible pressure vessel capable of achieving an ambient pressure of 20 atmospheres, and flow circuits for providing fuel and air to liquid injection systems. (Note the fuel injector used in these tests does not require an air supply.) A piping and instrumentation diagram of the facility is shown in Figure 2. Additional details about the facility can be given in [7].

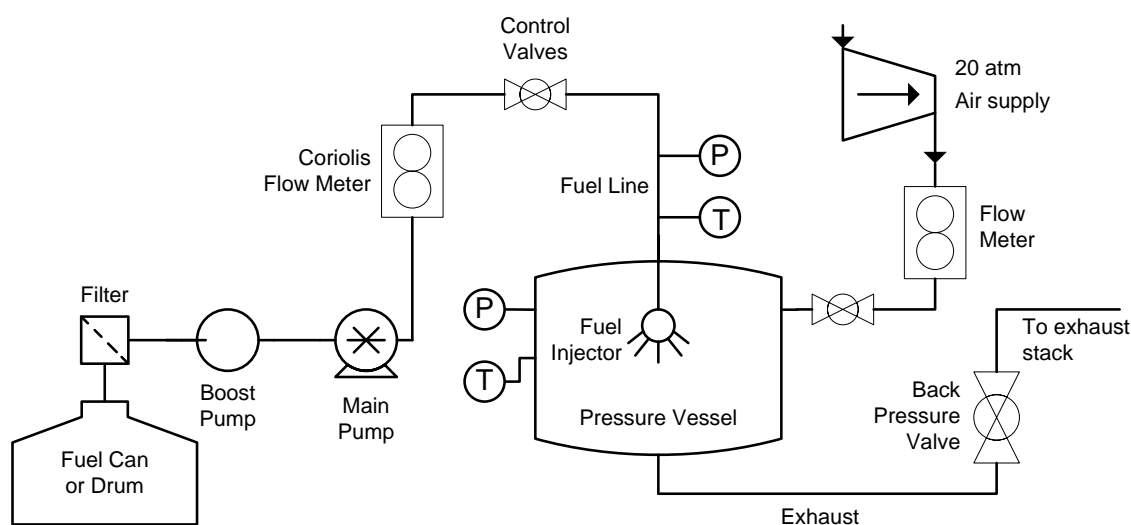
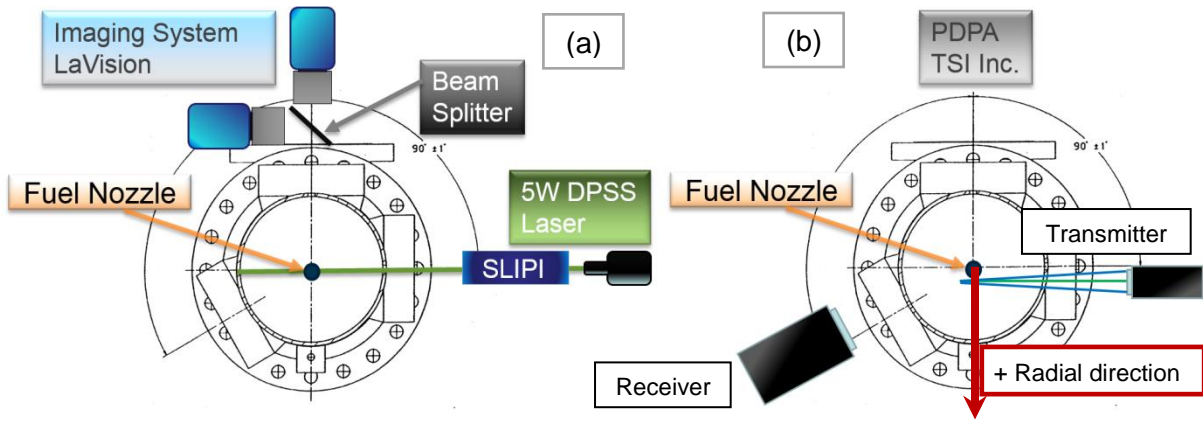


Figure 2. Piping and instrumentation diagram of the National Research Council High Pressure Spray Facility.

To gain a better understanding of the macro spray features, such as overall size and shape, conventional laser sheet images were collected. The images were captured using a Cannon 5D Mark II digital SLR, equipped with a Canon 24 – 105 f4.0 L-series lens. The spray was illuminated using a 5W DPSS laser, manufactured by UltraLasers, operating at 523 nm. The camera settings used were a shutter speed of 1/4000s, an f-stop value of 6.3, and ISO of 400. These were kept consistent for all flow conditions.

The components that make up the SLIPI LIF/Mie ratio-metric imaging system are shown in Figure 3 (a). They consist of two Imager ProX cameras controlled by a programmable timing unit (PTU), all from LaVision Inc. Each camera is equipped with the necessary filter to capture either the LIF or Mie signal. The Mie signal is an order-of-magnitude larger than its LIF counterpart, so a 90/10 beam splitter was used to achieve similar levels of signal intensity on both CCD’s. This approach also facilitates both cameras having an identical field of view. Previous work using this injector [8], showed it to be symmetrical, so only half of the spray was photographed in order to capture more of the downstream flow field, as well as maximize the use of the cameras’ chips. The lighting source employed was the same laser as the one used for the conventional images, save that the sheet forming optics also included a universal grating based SLIPI module. The system layout is shown in Figure 3 (a).

In order to calibrate the ratio-metric SLIPI images, spatially resolved Sauter-mean droplet diameters must be determined via another measurement technique. For this study, a TSI Inc. Phase Doppler Particle Analyzer (PDPA), was used. This off-the-shelf measurement system consisted of an optical receiver model RV2100, and a TM250 transmitter appointed with 500 mm lens and 2x beam expander. The transmitter and receiver were orientated 150 degrees apart, resulting the device having a velocity range of -225 m/s to 1125 m/s, and the ability to measure particle diameters from approximately 1 – 266 μm. A sketch of the PDPA setup is shown in Figure 3 (b). Additional information regarding the PDPA is presented in [5] and [8].



**Figure 3.** Top view of HPSF test section and optical diagnostics configuration.  
 (a) Layout of the SLIPI LIF/Mie Ratio-metric imaging system. (b) Orientation of the PDPA.

Three fluids were used during testing: nozzle calibration fluid (MIL-PRF 7024 E Type II, henceforth referred to as “MIL-C”), conventional Jet A (referred to “A-2”), and a high viscosity jet fuel (referred to as “C-3”). A brief description of the fuels is shown in Table 1. For detailed specifications on these fuels see [9]. In order to produce the LIF signal required for the ratio-metric images, the test liquids were doped with a fluorescing dye, pyromethene 597. This tracer fluoresces at 570 nm when excited by a 532 nm laser. For this application, approximately 0.01 g of dye per 100 L of fuel was needed to produce a sufficient fluorescent signal. Measuring this small quantity accurately poses a challenge, and as a result exactly identical amounts of tracer in each test fluids could not be achieved. To ensure the index of refraction, and physical properties of the fluids were unchanged by the dye, doped fuel samples were tested by an independent laboratory. In order to assess robustness as well as the range of applicability of the calibration an array of spray shapes and droplet sizes are needed. The test matrix used to achieve this is shown in Table 2. A larger set of spray characterization data has been presented in [8], however to be succinct, this paper will focus on only these 9 conditions since they offer a representative summary of this sprays behaviour.

**Table 1.** Summary of test fluids and properties

Fluid	Composition	Features	Viscosity at 25 °C [cSt]
MIL-C	Nozzle calibration fluid	Similar physical properties to A-2. Less flammable.	1.2
A-2	“Average” or “nominal” jet fuel - Jet A	Average properties.	1.7
C-3	64 vol% high viscosity jet fuel (JP-5) 36 vol% farnesane.	Very high viscosity jet fuel, (viscosity specification limit).	2.3

**Table 2.** Test Matrix

Condition #	Air Pressure - $P_3$ [atm]	Fuel Pressure - $\Delta P_f$ [kPa]	Fuel Mass Flow - $\dot{m}_f$ [g/s]
1	3.4	100	2
2	3.4	225	3
3	3.4	625	5
4	6.8	100	2
5	6.8	225	3
6	6.8	625	5
7	10	100	2
8	10	225	3
9	10	625	5

## Results and discussion

A selected sample of conventional laser sheet images are shown in Figure 4. They provide a qualitative overview of the sprays' general features, and demonstrate the overall trends as the type of fuel, ambient pressure, and fluid mass flow are changed. Figure 4 shows the reduction in spray's cone angle as the fuels become more and more viscous. Figure 4 also demonstrates that at higher flow rates, and correspondingly higher injection pressures, the nozzle does a better job of atomizing the fuel, the spray widens, and the viscosity trend becomes less pronounced. Figure 4 indicates how the sprays' features change with ambient pressure, with a progressive decrease in spray cone angle being observed. These results agree with the typical behaviour for simple pressure atomizers [10].

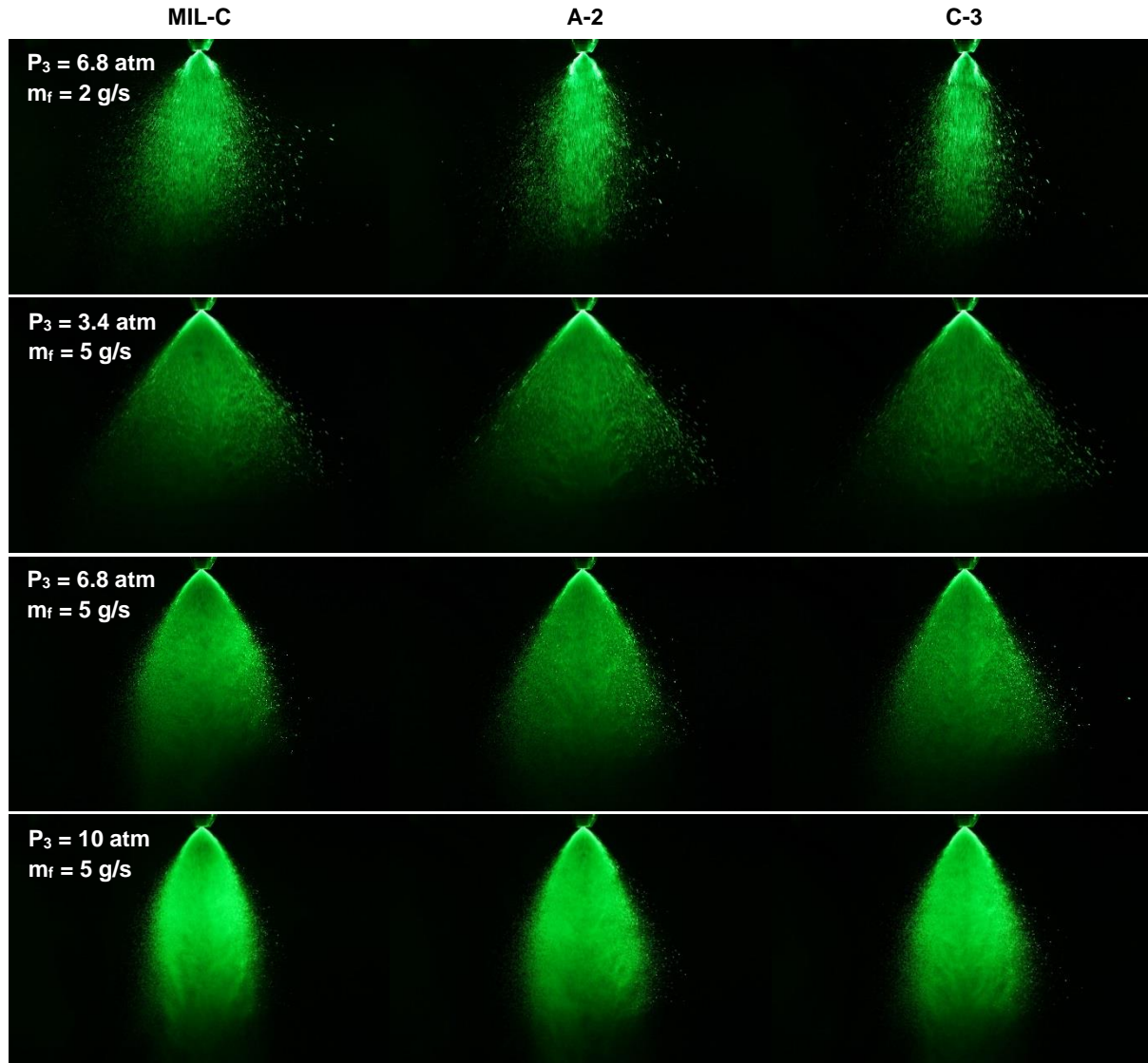


**Figure 4.** Conventional laser sheet images of the fuel sprays. Camera settings: 1/4000s, f/6.3, ISO-400.

The phase Doppler anemometry results are shown in Figure 5. All data was collected 50.8 mm from the nozzle's exit face. For the majority of the points taken, data rates were in excess of 1 kHz, with validation rates above 80%. The primary purpose for collecting these data was to calibrate the SLIPI LIF/Mie images, so only a brief interpretation of these results is given. A more in depth analysis can be found in [5]. In summary, the droplet sizes agree with expectation and show improved atomization with increased fuel flow. An indication of the spray's cone angle is also offered by noting the outermost point at which the PDA detects droplets. For the lower fuel flow conditions the data extends out to an average radius of 30 mm, while for the corresponding higher fuel flow conditions droplets are shown to exist at radial positions of 45 mm. This affirms the flow visualization results that show the cone angle widens as the fuel flow increases. All these results are in good agreement with similar measurements found in the literature [11], [12].

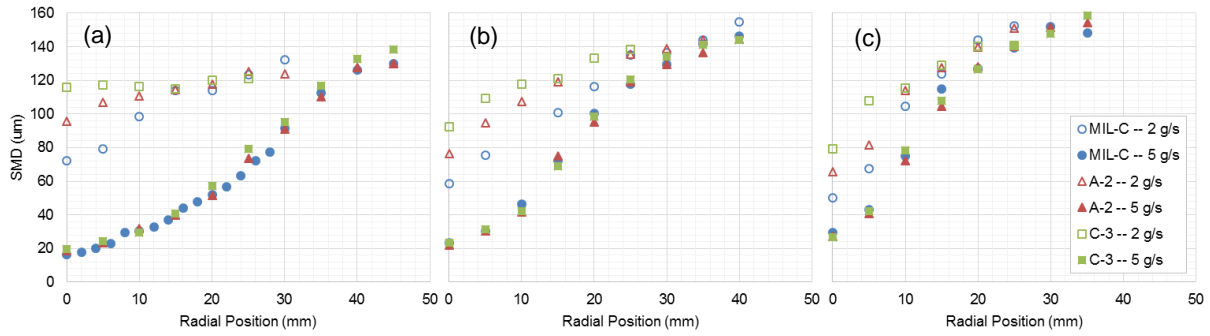


**Figure 5.** Sauter-mean diameter with radial position measured by phase Doppler anemometry at 50.8 mm from the nozzle face. (a)  $P_3 = 3.4$  atm, (b)  $P_3 = 6.8$  atm, (c)  $P_3 = 10$  atm

A sample SLIPI LIF/Mie ratio-metric image is shown in Figure 6(a). It is produced by dividing the pixel intensities in one SLIPI LIF image by those of one SLIPI Mie image. To produce the LIF and Mie SLIPI images with high enough levels of intensity the collection of 150 LIF and 150 Mie images was required. These 150 images are then averaged and processed with LaVision's DaVis software to produce what is shown in Figure 6(a). This SLIPI LIF/Mie ratio-metric image is said to be "un-calibrated" as the LIF/Mie pixel counts are proportional to the droplet SMD's, but the exact SMD's are unknown. Additional post processing has been applied to Figure 6(a) with the result shown in Figure 6(b). Residual noise in the image has been reduced by applying a 20 x 20 pixel median filter. This is equivalent to a 1 x 1 mm area in the flow. In this study, PDA has been used to calibrate the image. The white dots in Figure 6(b) show the corresponding location of these measurements in the image. The calibration curve shown in Figure 7(c) was used to convert the image shown in Figure 6(b) to produce a planar map the droplet's SMD, shown in Figure 6(c). This calibrated SLIPI LIF/Mie ratio-metric image contains a vast amount of spatially resolved droplet size information, and only requires a few seconds to capture. Producing a similar figure with PDA alone would require several hours, and given the cost of high pressure tests, represents an expensive proposition.

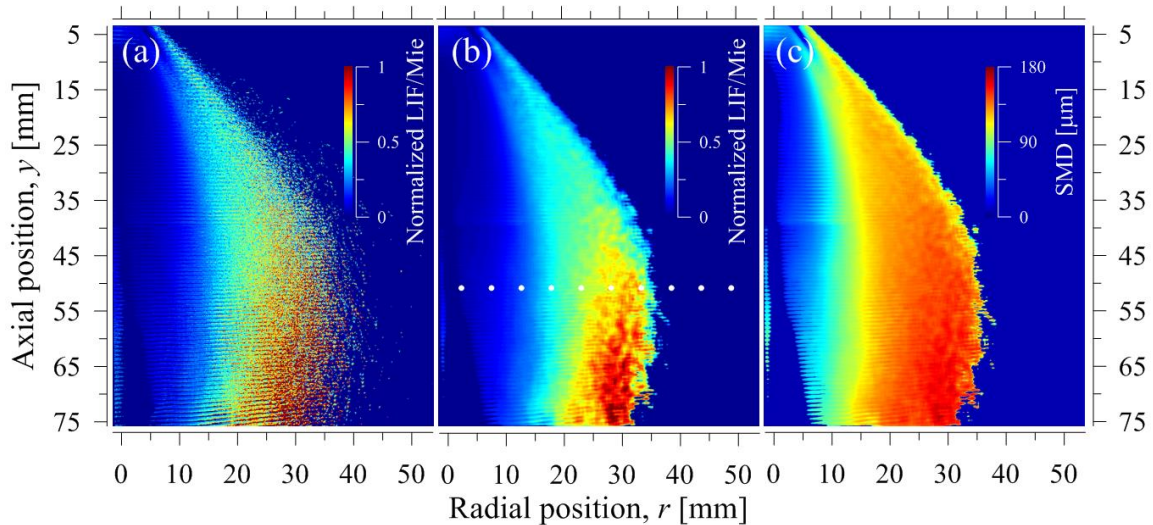


**Figure 6.** SLIPI LIF/Mie ratio-metric image of C-3 spray with geometric scale. Fuel flow 5 g/s,  $P_3 = 10$  atm. (a) Raw image. (b) Post processed image with location of PDA data. (c) Calibrated SMD Map

There are several noteworthy features in Figure 6(c). Firstly, because the SLIPI has removed the multiple scattered light effects, the hollow cone structure of the spray is well represented. Conversely however, the near nozzle region does not appear to have been captured accurately, with the image indicating an absence of fluid just downstream of the nozzle exit. This is likely due to the presence of fluid ligaments and non-spherical bodies in this location. LIF/Mie imaging presumes particle sphericity, so if this is not the case the ratio between the LIF and Mie signals will be heavily skewed, and will no longer follow a  $d^3$  to  $d^2$  relation. The image shows the SMD increases with axial position. As the jet travels downstream it expands and the droplets decelerate. This could cause droplet collisions and in turn conglomeration, leading to an increase in droplet diameters. In addition, the effects of droplet evaporation may also be contributing. Despite the tests being conducted at room temperature, some evaporation still occurs, which will eliminate the smaller droplets completely, resulting in a population with a larger SMD. These findings are consistent with other studies on similar injection systems [11], [12].

A summary of all the calibration data is shown in Figure 7. The x-axis of the figure shows the LIF/Mie ratio pixel count varied substantially between fuels. This is primarily a result of the dye concentration varying between tests, and demonstrates how sensitive this method is to this feature of the experimental set up. As such, if multiple calibrations are to be avoided, it is critical that the concentration of dye remain as consistent as possible through the experiment. Figure 7 also shows the calibration curves to have a distinct trend with pressure: higher ambient pressures result in larger SMD's for given LIF/Mie ratio pixel counts. This trend is present across all fuels and mass flows, and indicates that if the ambient pressure is changed substantially a corresponding calibration will be required.

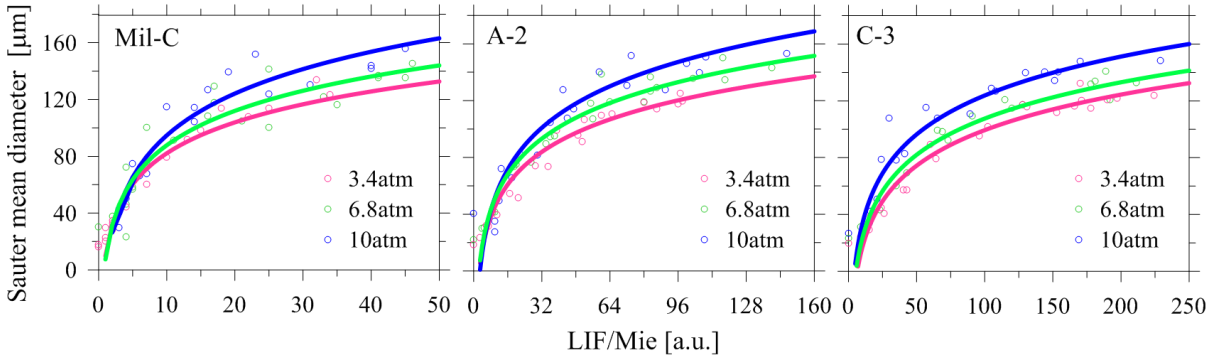


**Figure 7.** Calibration data and resulting calibration curves for SLIPI LIF/Mie ratio pixel counts for MIL-C, A-2 and C-3. Fuel flows of 2 g/s, 3 g/s and 5 g/s.  $P_3 = 3.4 \text{ atm}, 6.8 \text{ atm}$  and  $10 \text{ atm}$ .

There are a number of other experiment-specific particulars other than dye concentration that will affect the LIF/Mie ratio pixel count, such as laser power, camera sensitivity and exposure time, particle number density, as well as the algorithms which are used to process the raw images. All these factors, in addition to the inherent experimental uncertainties, will cause the calibration curves to vary from test to test. These variances are observed in Figure 7. Despite the numerous aforementioned factors that can affect pixel counts, all the curves generating in this study display a consistent shape, which can be described by a logarithmic function of the form:

$$SMD = A_1(\ln(x)) + A_2 \quad (1)$$

where  $x$  is the LIF/Mie ratio pixel count,  $A_1$  and  $A_2$  are empirical constants determined by the calibration. It's important to note that because the curve is not linear, interpreting un-calibrated images must be done with caution. An un-calibrated LIF/Mie ratio-metric image will still indicate where droplets are large and small, but the values will not be proportionally accurate.

To examine the effect of fuel mass flow on the calibration curve, the calibration data at each ambient pressure is plotted in Figure 8. For clarity, only fluid C-3 is presented, as all test liquids portray the same trend. Figure 8 indicates that the variance in calibration curve due to changes in fuel mass flow is less than the inherent uncertainties in the data as discussed above. This shows, that provided the dye concentration and ambient pressure are unchanged, the calibration curves were found to be consistent with liquid mass flow. This is a positive finding, as it means for experiments in which there is no need to change test fuel or ambient pressure, a limited amount of calibration data will be required, greatly reducing time and cost.

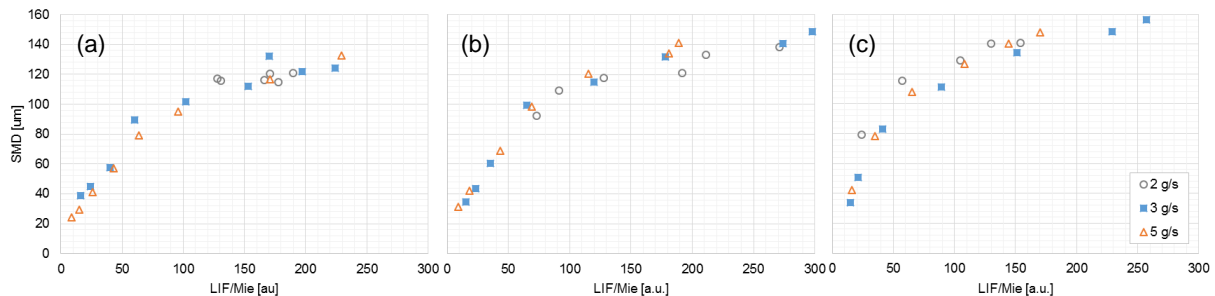


**Figure 8.** Calibration data for SLIPI LIF/Mie ratio pixel counts for test fluid C-3. (a)  $P_3 = 3.4 \text{ atm}$ , (b)  $6.8 \text{ atm}$  and (c)  $10 \text{ atm}$ .

The corresponding calibration curves shown in Figure 7 were used to produce the SMD maps found in Figure 9. This chart gives a detailed comparison of how the A-2 fuel spray changes with ambient pressure. In addition to showing the increase in droplet size, the axial and radial position where the large droplets are forming is also visible.

These images also provide details about the spray's inner and outer cone angles, which could be calculated with additional post processing. The large amount of information contained in these images demonstrates this diagnostics commanding potential to gather large quantities spray characterization data quickly.

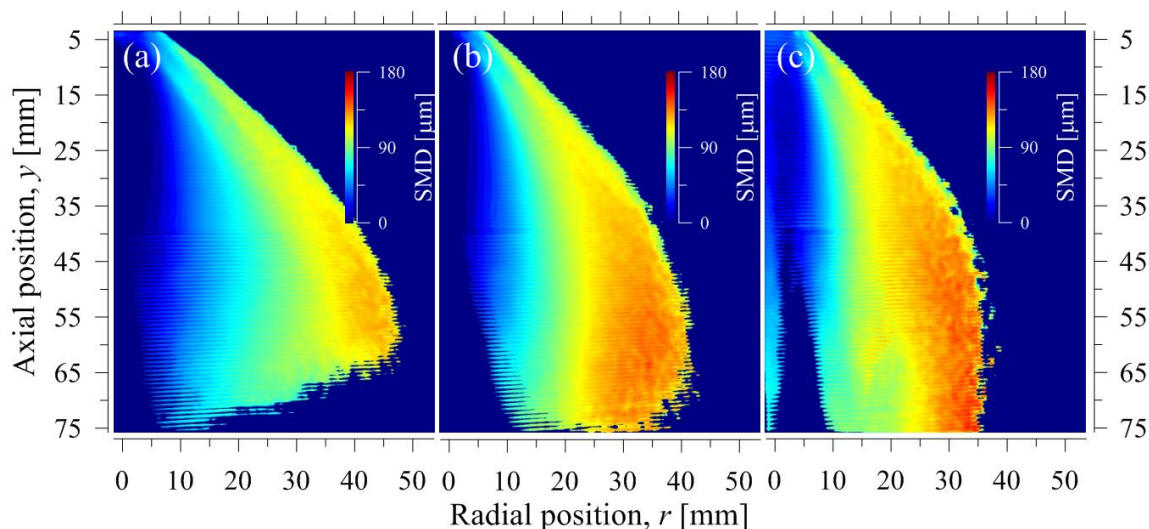


**Figure 9.** Calibrated SMD maps for A-2 fuel spray. Fuel flow 5 g/s. (a)  $P_3 = 3.4$  atm, (b)  $P_3 = 6.8$  atm, (c)  $P_3 = 10$  atm.

### Conclusions and future work

A procedure for using PDA to calibrate SLIPI LIF/Mie ratio-metric images of a spray produced by a simple pressure atomizer has been explored. Both the PDA and LIF/Mie data show the same overriding trends in this spray: atomization improves with increasing fuel flow rate, and degrades with increasing ambient pressure. Conventional laser sheet images were also collected in order to help support the observations made using the other measurements. The calibration data has been presented for three ambient pressures (3.4 atm, 6.8 atm and 10 atm), using three test liquids (conventional jet fuel, alternative jet fuel, and a nozzle calibration fluid), at flow rates of 2 g/s, 3 g/s and 5 g/s. Calibration curves were found to be indifferent to fuel flow rate, but were observed to have a dependence on ambient pressure. This suggests that if tests are being performed over a range of ambient pressures, multiple calibrations will be required. The results also showed that LIF/Mie ratio pixel counts varied substantially between fuels. This is attributed to variations in the fluorescing dye concentrations. All calibration curves follow the same general profile which can be approximated by a logarithmic function. As such, if dye concentrations are kept consistent between tests, a small number of PDA data points can potentially be used to calibrate a large number of LIF/Mie ratio-metric images, provided the calibration data covers the full range of droplet sizes. Additional work is still required to refine this method, and in order to improve the results in future experiments superior cameras will be employed. In addition to this, replacing the continuous wave laser with a higher power pulsed option will allow for faster exposures, which should help improve the quality of the images. That in-turn will reduce noise in the data, resulting in more consistent calibration curves.

### Nomenclature

$d$	Droplet diameter
$P_3$	Test section pressure [kPa]
$\Delta P_f$	Differential fuel pressure [kPa]
$m_f$	Mass flow of fuel [g/s]
$r$	Radial position [mm]
$x$	LIF/Mie ratio pixel count
$y$	Axial position [mm]
CCD	Charged Couple Device
FN	Flow Number
HPSF	High Pressure Spray Facility
LIF	Laser Induced Fluorescence
NJFCP	National Jet Fuel Combustion Program
NRC	National Research Council
P&ID	Piping and Instrumentation Diagram
PDA	Phase Doppler Anemometry
PDPA	Phase Doppler Particle Analyzer

PTU	Programmable Timing Unit
SLIPI	Structured Laser Illumination Planar Imaging
SLR	Single-Lens Reflex
SMD	Sauter-Mean Diameter (D32)

## References

- [1] Berrocal E., Kristensson E., Richter M., Linne M. and Aldén M. (2008), Application of structured illumination for multiple scattering suppression in planar laser imaging of dense sprays, *Opt. Express*, 16, 17870-17881.
- [2] Berrocal E., Kristensson E., Hottenbach P. et al. *Appl. Phys. B* (2012) 109: 683.  
<https://doi.org/10.1007/s00340-012-5237-9>
- [3] Berrocal E., Kristensson E., Hottenbach P., Grünefeld G., and Aldén M., Quantitative laser imaging of a non-reacting diesel spray using SLIPI. ILASS Americas, 23rd Annual Conference on Liquid Atomization and Spray Systems, Ventura, CA, May 2011
- [4] Mishra, Y. M., Kristensson E., Berrocal E. (2015). Reliable LIF/Mie droplet sizing in sprays using structured laser illumination planar imaging. *Optics Express*, 22:4480-4492.
- [5] Corber A., Chishty W.A., Patrizio V. (2019), Planar LIF/Mie Ratio Droplet Sizing Using Structured Laser Sheet Imaging at Elevated Ambient Pressures, Proceedings of Global Power and Propulsion Society Technical Conference, Zurich, Switzerland, GPPS-TC-2019-0048.
- [6] Buschhagen T., Zhang R. Z., Bokhart A. J., Gejji R. M., Naikz S. V., Lucht R. P., Gore J. P., Sojka P. E., Slabaugh C. D., Meyer S. E. (2016). Effect of Aviation Fuel Type on Fuel Injection Conditions on Non-reacting Spray Characteristics of a Hybrid Airblast Fuel Injector. 54th AIAA Aerospace Sciences Meeting AIAA SciTech Forum, (AIAA 2016-1154).
- [7] Corber A. (2007). A Preliminary Investigation of Flow Scaling for Injector Characterization. ILASS Americas, 20th Annual Conference on Liquid Atomization and Spray Systems, Chicago, IL, May 2007.
- [8] Corber A., Rizk N., Chishty W. A. (2018). Experimental and Analytical Characterization of Alternative Aviation Fuel Sprays Under Realistic Operating Conditions. Proceedings of ASME Turbo Expo 2018, Oslo, Norway, GT2018-75574.
- [9] Colket M. , Heyne J., Rumizen M., Gupta M., Edwards T., Roquemore W. M., Andac G., Boehm R., Lovett J., Williams R., Condevaux J., Turner D., Rizk N., Tishkoff J., Li C., Moder J., Friend D., Sankaran V. (2017). Overview of the National Jet Fuels Combustion Program. (AIAA 2017 55:4, 1087-1104)
- [10] Lefebvre A. H. and McDonell V. G (2017) *Atomization and Sprays*. CRC Press: Taylor & Francis Group
- [11] McDonell V. G., Samuelsen G. S., Wang M. R., Hong, C. H. and Lai W. H. (1994). Interlaboratory comparison of phase Doppler measurements in a research simplex atomizer spray, *Journal of Propulsion and Power*, Vol. 10, No. 3 (1994), pp. 402-409.
- [12] McDonell V. G., Samuelsen G. S. (1995), An Experimental Data Base for the Computational Fluid Dynamics of Reacting and Nonreacting Methanol Sprays. *ASME. J. Fluids Eng.* 1995;117(1):145-153.  
doi:10.1115/1.2816804.

## Acknowledgements

The financial support for this study was provided by the Aeronautical Product Development Technologies program of National Research Council Canada and Transport Canada. The authors gratefully acknowledge the technical contributions of Mr. Daniel Arbiq and Mr. Nicholas Charest from of National Research Council Canada. The authors are indebted to the US AFRL for supplying the test fuels, as well as Edouard Berrocal and Elias Kristensson from Lund University for their assistance with the SLIPI set up and data reduction.